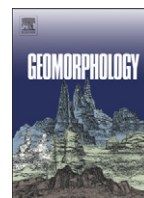




Contents lists available at ScienceDirect

Geomorphology

journal homepage: www.elsevier.com/locate/geomorph

Comparison of short-term seacliff retreat measurement methods in Del Mar, California

Adam P. Young ^{a,*}, R.E. Flick ^a, R. Gutierrez ^b, R.T. Guza ^a

^a Integrative Oceanography Division, Scripps Institution of Oceanography, University of California San Diego, 9500 Gilman Dr., La Jolla, CA, 92093-0209, USA

^b The University of Texas at Austin, 1 University Station, Austin, TX, 78712, USA

ARTICLE INFO

Article history:

Received 31 March 2009

Received in revised form 23 June 2009

Accepted 23 June 2009

Available online xxx

Keywords:

Coastal erosion

Seacliff retreat

Southern California

Change detection

LiDAR

ABSTRACT

Seacliff retreat has been variously characterized as the recession rate of the cliff top, of the cliff base, and as the bulk recession rate based on volumetric changes of the entire cliff face. Here, these measures of retreat are compared using nine semi-annual airborne LiDAR (Light Detection And Ranging) surveys of southern California seacliffs. Changes in the cliff base location (where the steeply sloping cliff face intersects the beach) include cliff retreat owing to basal erosion, but also reflect changes in beach sand level and basal talus deposits. Averaged over the 2.5 km alongshore study span, the cliff base actually prograded seaward about 12 cm during the 4-year study. Cliff top change was dominated by few, relatively large (several meters) localized retreats. Cliff face changes, that include failures and deposits anywhere on the cliff profile, had a relatively small mean magnitude compared to cliff top changes and were more widely distributed alongshore. However, the similar alongshore averaged, cumulative cliff top and net bulk cliff face end-point retreat (14 and 19 cm, respectively) suggest that mean cumulative cliff top retreat can potentially be a viable surrogate for mean net cumulative cliff-wide erosion (and vice versa) over relatively short time periods. Cliff face erosion occurred repeatedly at some locations, confirming the presence of seacliff erosion hot-spots during the study period.

© 2009 Elsevier B.V. All rights reserved.

1. Introduction

Seacliff retreat, important to coastal management, is often estimated using the recession of the cliff top or cliff base obtained from aerial photographs, topographic maps, or in situ surveys (e.g. Jones and Williams, 1991; Wilcock et al., 1998; Benumof and Griggs, 1999; Moore et al., 1999; Budetta et al., 2000; Hapke and Richmond, 2002; Pierre and Lahousse, 2006; Dornbusch et al., 2008; Greenwood and Orford, 2008). Recently, three-dimensional high resolution maps derived from LiDAR have been used to estimate the cliff face bulk retreat, defined as the volumetric change (measured by differencing successive digital elevation models) divided by the cliff height and the alongshore width of a cliff section (Young and Ashford, 2006a,b).

Cliff top, base, and face change estimates can differ significantly over short time periods. For example, wave action can cause cliff base retreat, but no cliff top change (Fig. 1A). Mid-cliff face erosion can occur without changes to the cliff top or base (Fig. 1B). Alternatively, a cliff top failure may result in significant cliff top recession and no change at the cliff base if the talus is removed by wave action prior to subsequent data collection (Fig. 1C). When talus deposits are incompletely removed between surveys, the cliff base appears to accrete (Fig. 1D, E). Additionally, the cliff base location changes when

the beach sand level at the cliff base changes (Fig. 1F, an increase in beach sand level causes retreat of the estimated cliff base location).

Although these estimates will converge over long time periods, short-term, seasonal estimates provide insight into cliff retreat processes (e.g. the relative importance of higher than usual rainfall or waves). Here, changes in the cliff top, cliff base, and cliff face, estimated using nine semi-annual airborne LiDAR surveys spanning four years are compared.

2. Study area

The studied 2.5 km reach of seacliffs in Del Mar, California (Fig. 2B), on average 18 m high with approximately 45° slope, are cut into uplifted marine terraces. The lower cliff consists of the Del Mar Formation, an Eocene sedimentary deposit composed of sandy claystone interbedded with coarse-grained sandstone (Kennedy, 1975). Near the middle of the study area, the Del Mar Formation is overlain by permeable sandy Pleistocene terrace deposits (Fig. 2C). The Del Mar Formation is relatively impermeable, resulting in perched groundwater and sapping at the interface with terrace deposits. The cliff face experiences weathering, desiccation, sheet erosion, and rilling, while the cliff base is subject to wave action. Typical beach width ranges from 30 to 70 m, and fluctuates seasonally with wider beaches in summer. During winter, the eroded beach permits direct wave attack at the cliff base when elevated tides coincide with large

* Corresponding author. Tel.: +1 858 822 3378; fax: +1 858 534 0300.

E-mail address: adyoung@ucsd.edu (A.P. Young).

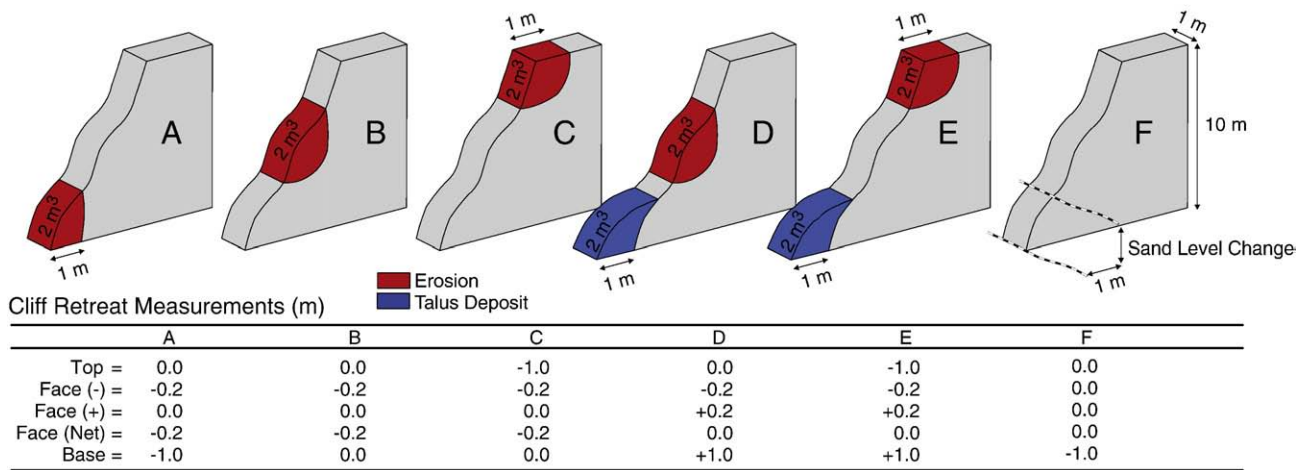


Fig. 1. Interpretations of idealized cliff changes using the three different retreat estimates.

wave events. Subaerial and marine erosional processes result in long-term cliff top retreat rates estimated at 5–20 cm/yr (Benumof and Griggs, 1999; Moore et al., 1999; Young, 2006; Hapke and Reid, 2007). The North County Transit District railroad, currently situated on the

cliff top within a few meters of the cliff edge, has been threatened by past cliff failures (Kuhn and Shepard, 1984). Portions of the cliff base stabilized with wooden and concrete seawalls (Fig. 2D) were identified with oblique photographs (California Coastal Records Project, 2008).

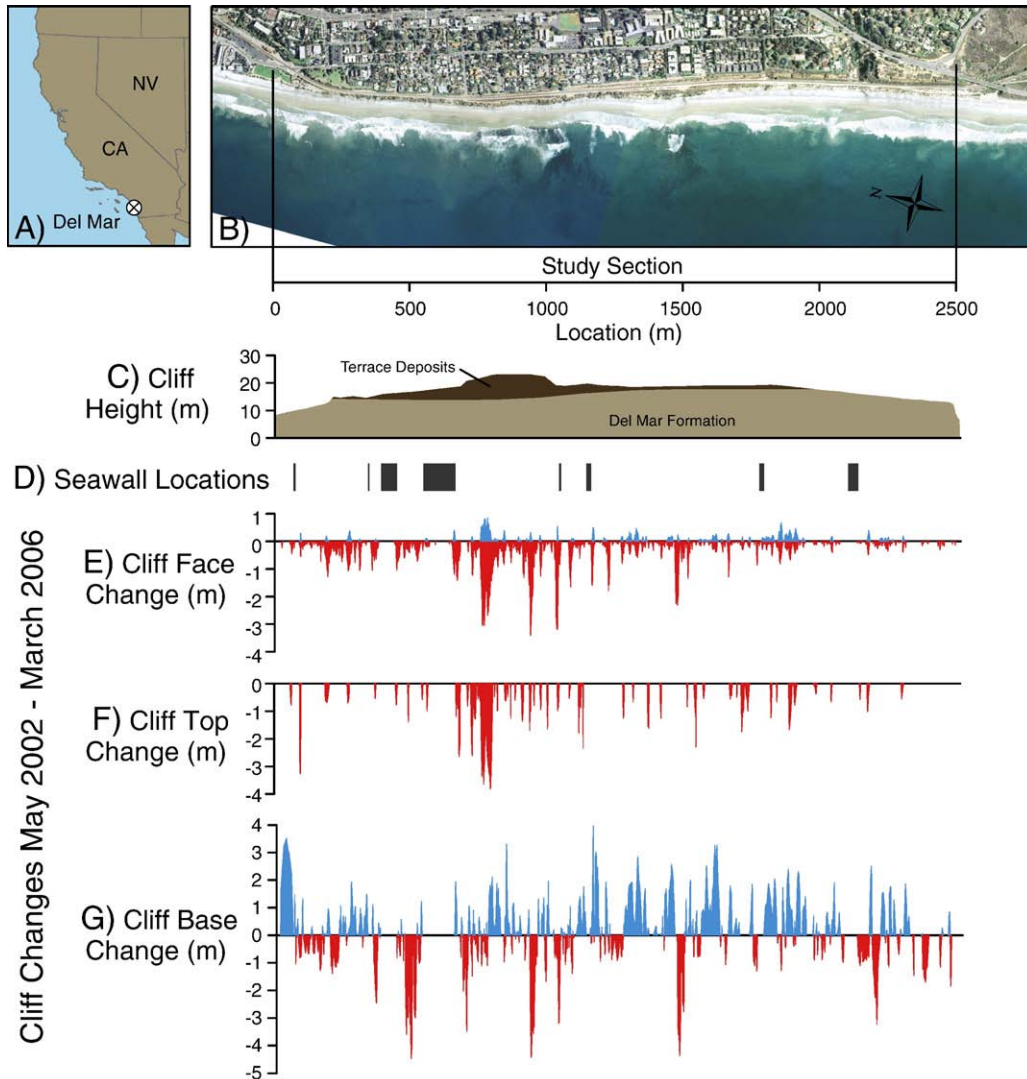


Fig. 2. A and B) Study location maps, C) cliff height and composition, D) major seawall locations, and cumulative (4 yr) changes of the cliff (E) face, (F) top, and (G) base versus alongshore location.

The seacliffs are exposed to waves generated by local winds and distant storms in both hemispheres. During winter, swell from the North Pacific and Gulf of Alaska are most energetic, whereas swell from the South Pacific dominates in summer. Waves reaching southern California cliffs undergo a complex transformation, and “shadows” of the Channel Islands create strong alongshore variations in wave height. The seasonal cycle in the Del Mar region has maximum wave energy in winter. Historical data indicates regional wave heights during the study period (May 2002–March 2006) were typical.

San Diego's semi-arid Mediterranean climate is characterized by dry summers and occasionally wet winters, with 85% of rainfall occurring from November through March. Annual precipitation amounts vary from about 10–60 cm, and average 25 cm. Rainfall in the region tends to be episodic and several centimeters of rain often fall over a few days. The study period was relatively dry, except for the wet winter of 2004–2005 when winter storms delivered about 56 cm of rain, resulting in significant coastal landsliding.

3. Methods

Airborne LiDAR data was collected each spring and fall from May 2002 through March 2006 with an Optech Inc. Airborne Laser Terrain Mapper 1225. The nine surveys yielded eight time intervals of cliff change. Four passes during each survey at an altitude of 300–1000 m provide a point density of approximately 3 points/m² on the cliff. LiDAR data were processed into 0.5 m² resolution digital elevation models (DEM) using the second of two LiDAR returns (the most representative of the ground surface) and a “natural neighbors” interpolation. Cliff height (Fig. 2C) and the beach sand elevation near the cliff base were obtained from the DEMs.

3.1. Cliff top and cliff base changes

Cliff base positions were identified manually from the DEM as the location of the slope break between the beach and cliff face. Similarly, cliff top location was defined as the slope break between the cliff face and the cliff top. For this particular cliff section, the break in slope is relatively easily identified and generally free of vegetation. However identifying cliff top and base positions may be difficult in other cliff sections lacking a clear break in slope or because of obstructions such as vegetation. For each survey, the digitized line (cliff top or base) from the previous survey was used as a baseline, and adjusted where new changes occurred. Changes were estimated on cross-shore transects spaced at 1 m intervals alongshore.

Automated cliff top and cliff base extraction methods (i.e. Liu et al., 2009) were not employed because these methods can induce significant errors when measuring relatively small changes in cliff top and base positions. For example, Liu et al. (2009) found average planimetric differences ranging from 2.5 to 4.2 m between manually digitized lines and automated extracted lines from airborne LiDAR data. Although errors of this magnitude may be negligible when cliff retreat is large, the potential error associated with automated algorithms exceeds the average retreat magnitude in this short-term study and therefore were not used.

3.2. Cliff face changes

Digital change grids (DCG), estimated by differencing successive DEMs, show both negative (erosion) and positive (accretion, talus deposits) changes. Sources of DCG error include the basic LiDAR observations, spatial interpolation, and vegetation. The vertical root mean square difference between two surveys (RMS_z , Federal Geographic Data Committee, 1998), a measure of the total error, was estimated at 19 cm using fixed sloped surfaces.

The DCGs were filtered and edited to remove noise and erroneous data. First, all grid cells with vertical change less than 38 cm (twice the

RMS_z error) were neglected. Next, a minimum topographic footprint was imposed, requiring at least 10 connected cells of positive or negative change, thus enforcing a minimum change area of 2.5 m². This filtering identifies individual landslides and talus deposits with a minimum volume of about 1 m³ (if all 10 cells had 38 cm of change). In practice, the minimum volume was approximately 2 m³. Finally, the filtered DCG data were edited visually to remove spurious changes caused by vegetation. Manual editing was employed rather than automated algorithms designed to remove vegetation from LiDAR because these algorithms sometimes also remove valid cliff points where cliff geometry is complex.

Cliff face changes were separated into negative (cliff and talus erosion) and positive (talus deposits) volumetric changes and then evaluated in 1-m wide (in the alongshore direction) cliff compartments. Dividing the volumetric compartment changes by the cliff height and compartment width (1-m) yielded bulk negative and positive cliff face changes. The overall method is automated except for the manual removal of spurious changes caused by vegetation or other artifacts.

The calculated change volumes underestimate the actual erosion because only relatively large volume (>2 m³) and large footprint (>2.5 m²) slides are detected. The neglected small events may play an important role in short-term seacliff evolution (Rosser et al., 2005; Young and Ashford, 2007), and their volume contribution for the study period is unknown. However, previous studies in the area (Young and Ashford, 2007), suggest the volume contribution of these small events is less than 30% of the total eroded volume (Young et al., in press).

4. Results

4.1. Beach sand levels

Sand level changes measured at the cliff base ranged from 0 to 1.5 m, and were relatively small with an average absolute magnitude of 22 cm. Only 20% of the changes were greater than 35 cm. Over the entire beach face, normal seasonal change is observed (not shown), with elevated sand levels in summer (Aubrey et al., 1980). Interestingly, beach elevation changes at the cliff base were not seasonal. Average sand levels at the cliff base decreased in all time intervals except during the winters of 2003–2004 and 2005–2006. Cobble berms, which are ephemeral features in the region, occasionally build up at the cliff base during winter months and probably contributed to some of the measured beach elevation changes at the cliff base.

4.2. Cliff base changes

Cliff base change is strongly variable alongshore, and change of both signs was observed, both in a given time interval, and cumulatively (Fig. 2G). Alongshore-averaged cliff base changes were negative, except during the summer of 2002 and (especially) the winter of 2004–05 (Fig. 3A). The cumulative (over 4 years) cliff base change in 1-m sections ranged from –4.5 to +4.0 m, with an alongshore average of +12 cm. Cliff base changes were relatively widespread, comprising up to 37% of the study area during a single interval (Fig. 3D). The alongshore average of nonzero changes ranged from –0.5 to +0.7 m over the 8 time intervals (Fig. 3C). The largest change in a 1-m section during any time interval was +7.5 m (accretion), caused by a relatively large and clearly identifiable talus deposit (Fig. 4A).

4.3. Cliff top and cliff face changes

The cumulative cliff top retreat in 1-m sections ranged from 0.0 to –3.8 m (Fig. 2F), with an alongshore average of –14 cm. Changes occurred along less than 8% of the cliff top during any time interval

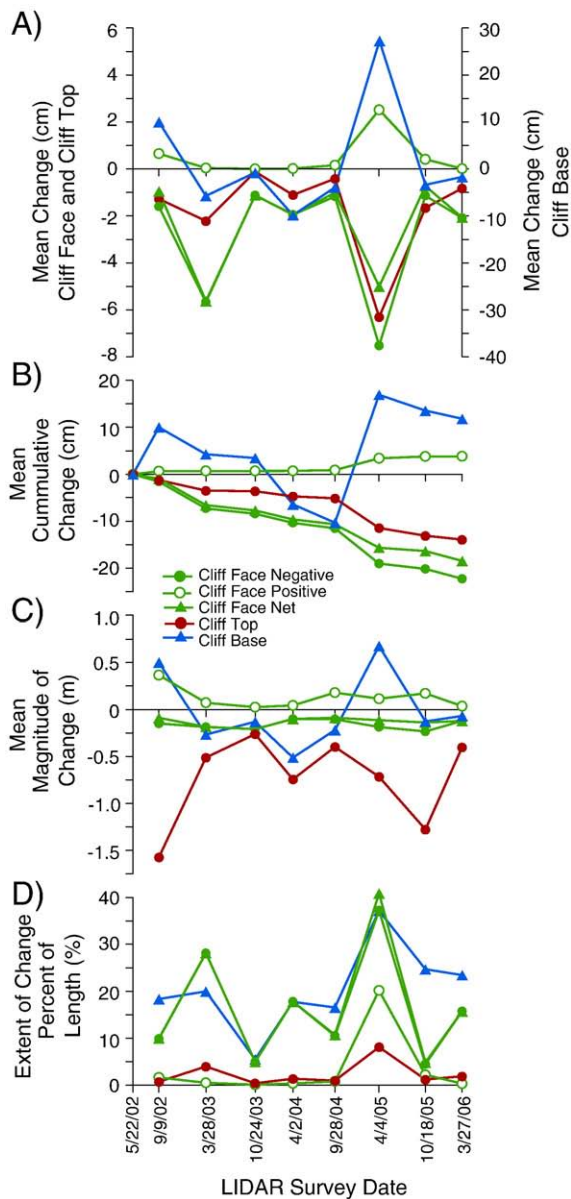


Fig. 3. Seacliff changes over the 2.5 km study area during each time interval, (A) mean change, note the change magnitude scale (y-axis) is different for the cliff base, (B) cumulative mean change, (C) mean change magnitude (zero changes neglected), and (D) percent of 1-m cells with nonzero change (number of 1-m cells with change/total number of 1-m cells).

(Fig. 3D). The alongshore averaged magnitude of nonzero changes ranged from -0.3 to -1.6 m over the 8 time intervals (Fig. 3C). The largest change in a 1-m section, during any time interval, was -3.8 m (Fig. 4C).

The cumulative cliff face change in 1-m sections ranged from -3.4 to $+0.9$ m, with an alongshore average of -22 cm, $+4$ cm, and -19 cm for the cliff face negative, positive, and net change, respectively. Positive changes (primarily talus accretion) occurred in less than 2% of the study length except during the winter of 2004–05 when positive change occurred in over 20% of the alongshore span (Fig. 3D). Negative changes were more spatially extensive and ranged from 5 to 37% of the study length during individual time intervals (Fig. 3D). The alongshore average magnitude of nonzero cliff face changes ranged from -10 to -23 cm, and $+3$ to $+37$ cm, for negative and positive change, respectively (Fig. 3C). The largest change in a 1-m section during any time interval was -2.2 m and 0.8 m for cliff face erosion and accretion, respectively.

Cliff face erosion (negative change) was spatially widespread, while cliff face positive and cliff top changes were relatively localized (Fig. 3D). Mean magnitudes of cliff top change (locations of zero change neglected) varied seasonally between -0.5 and -1.5 m, while the mean cliff face measurements were comparatively small (Fig. 3C). Cliff face changes occurred without cliff top or base change when the cliff material was eroded from the central portion of the cliff rather than cliff top or cliff base, and the associated talus was eroded before it could be measured. At all locations with nonzero cliff top retreat, cliff face retreat was also observed.

5. Discussion

5.1. Beach sand levels

The vertical elevation of beach sand at the cliff base limits the portion of the cliff base that can be surveyed, and thus contributes to changes in cliff base horizontal location. Measured horizontal cliff base locations are most effected by sand levels at locations with relatively low cliff base (or talus) slope angles. Although the average beach sand level change magnitude was relatively small and did not result in perceptible cliff base change at most locations, large sand level changes did cause spurious cliff base change measurements in some instances. For example, at one location (where no talus deposition occurred) the sand level was lowered by about 1.0 m, exposing more of the cliff and resulted in a $+1.5$ m (seaward) change of the cliff base. However, the majority of the observed large magnitude (>1.0 m) cliff base displacements coincided with locations of new talus deposition and talus erosion. The maximum horizontal change caused by sand level change is approximately 2 m, estimated as the maximum change in beach elevation (≈ 2 m) divided by $\tan \alpha$, where α is equal to the slope at the cliff base ($\approx 45^\circ$).

Beach sand level changes can also affect cliff face measurements. For example, if the beach sand level increases prior to talus deposition, the talus volume estimate will include the accreted volume of sand under the talus. This affect is probably relatively small, because most new talus deposits were removed by wave action between surveys (cliff face positive changes \ll cliff face negative changes, Fig. 4F), and if the talus was not removed only a small portion was generally located on the beach (talus is often deposited on the lower cliff face, Fig. 4A). Furthermore, the average magnitude of beach change was smaller (22 cm) than the vertical change threshold (38 cm). However, these small errors will increase with larger sand level fluctuations. The maximum volume error from fluctuations in sand levels equals approximately the area of talus on the beach multiplied by the maximum expected change in beach sand elevation.

5.2. Cliff base changes

Unlike the cliff top, cliff base location changes are not dominated by retreat (negative change). Cliff base location changes (identified here as the break in slope between the cliff and beach) are a combination of spurious changes resulting from beach sand level changes, talus deposition and removal (Fig. 4A, B), and real cliff base retreat. At much longer time scales (possibly several decades, based on historical erosion rates), cliff base retreat is larger than changes from either talus or beach sand levels, and this method will yield estimates of in situ cliff base erosion.

5.3. Cliff top and cliff face changes

Cliff top retreat was dominated by localized large events, and was the most episodic of the retreat estimates, with a mean magnitude of cumulative cliff top change (-82 cm, locations of zero change neglected) six times greater than mean cumulative change (-14 cm, including all locations). The cliff top and cliff face magnitude-

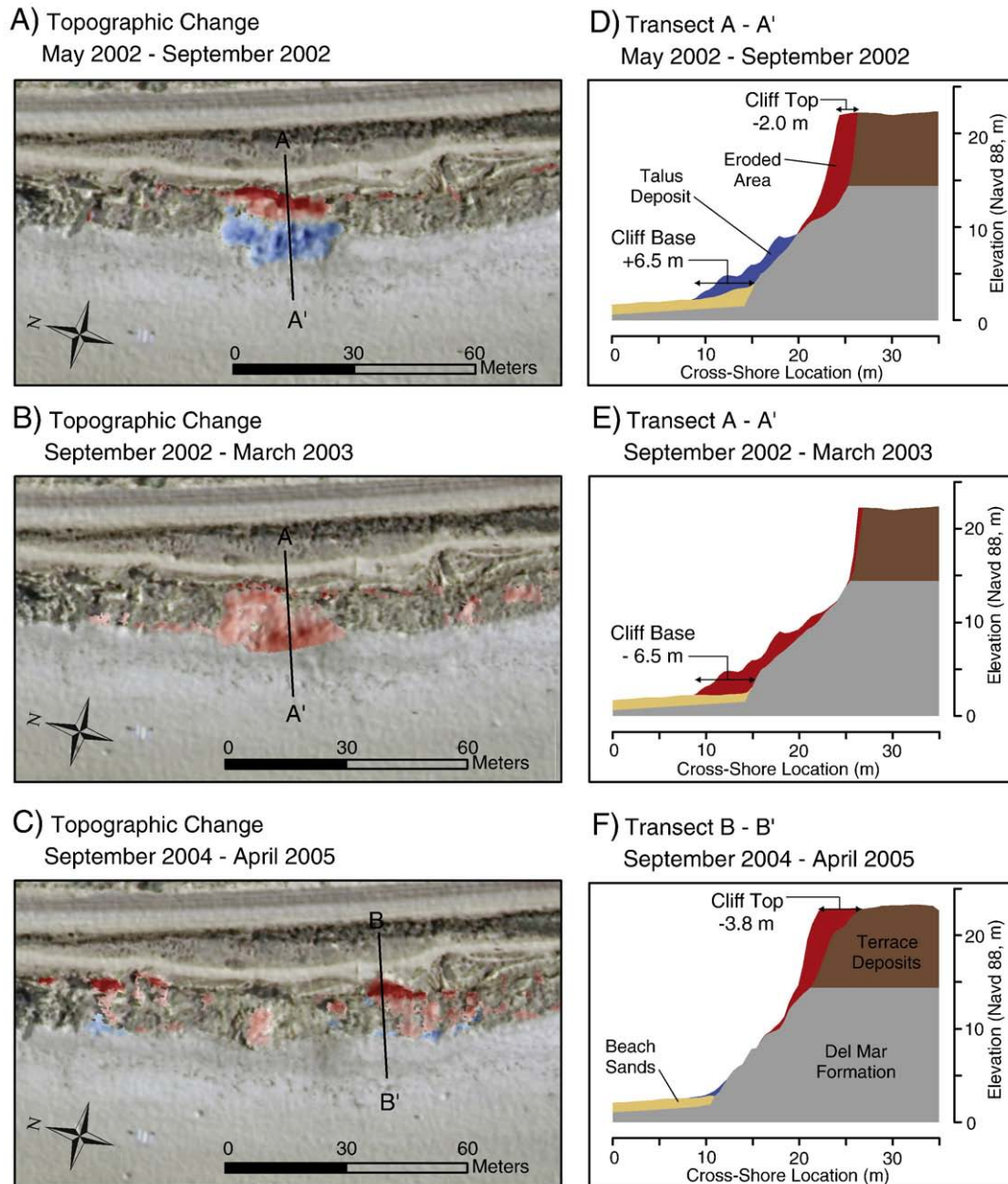


Fig. 4. Changes over a 120 m cliff section during 3 time intervals, where red and blue indicate erosion and accretion, respectively. A) Large upper cliff landslide and associated talus deposit. B) Next survey shows both continued cliff erosion, and erosion of the talus deposit in panel A. C) The upper cliff landslide associated with the largest cliff top retreat, -3.8 m. The talus was almost all eroded before the April 2005 survey. (D, E, F) Cliff profiles associated with panels A, B, C.

frequency distributions differ; 50% of cliff top changes were larger than -50 cm, compared with 6% for cliff face change. During most of the study period (an exception is the winter of 2004–2005), negative (erosional) cliff face changes were much more extensive than positive (depositional) changes, indicating that the available wave action was sufficient to erode talus deposits.

Although cliff top and face change differs significantly, there are similarities. For example, mean cumulative cliff face (negative and net) and top changes are correlated ($r^2 > 0.9$), whereas the cumulative cliff base changes are uncorrelated with the top and face (Fig. 3B). The cliff face and cliff top both show seasonality, with relatively more change during winter than summer (Fig. 3A), whereas cliff base changes are not seasonal. All methods recorded relatively extensive changes during the winter of 2004–05, and limited change during summers (Fig. 3D).

5.4. Geomorphic perspective

The seasonality of cliff top and cliff face changes reflects the seasonal variation of both wave energy and rainfall, which have greater potential for cliff erosion during the winter months. Our measurements of cliff base changes encompass a variety of processes, some of which can oppose each other during a given time interval. For example during winter months a large landslide deposit causes the cliff base to move seaward, while wave erosion of the cliff base produces landward movement. This type of opposition contributed to the lack of seasonality in observed cliff base changes.

The wet winter of 2004–2005 had a relatively profound affect on the Del Mar seacliffs, with the absolute maximum mean cliff face, cliff top, and cliff base changes all occurring during this winter (Fig. 3A). Rainfall triggered numerous coastal landslides and initiated erosion

through other subaerial processes ultimately eroding a total volume of about 3500 m³. Available wave action was insufficient to remove the talus, and approximately 1/3 of the total eroded volume (1150 m³) remained as talus at the end of the winter. The remaining talus during this time interval was more than double the volume in all other time intervals combined, and probably temporarily protected in situ cliff material from wave-induced erosion. As these talus deposits are reworked by future wave action, the erosion rates will probably be elevated, because talus is much more easily eroded than in situ cliff material.

Cliff top retreat reduces the overall cliff slope, while cliff base and cliff face erosion (not concentrated at the cliff top) cause overall slope steepening, thus reducing overall cliff stability. During the study period, 50% of both cliff top and cliff face failures were preceded by cliff face erosion at the same location during the previous year. This effect was cumulative over the study period and led to the development of localized erosional hot-spots. At some locations hot-spots persisted for the duration of the study period, with cliff face erosion occurring in 7 of the 8 time intervals. However, cliff face erosion did not necessarily lead to cliff top failure, and only 18% of cliff face erosion locations were followed by a cliff top failure, probably because of the relatively short study time period and the highly episodic nature of cliff top retreat. Over longer time periods, these concepts can be used to develop a seacliff erosion hazard index, defined as the difference between cliff top and cliff face erosion. For example, as the cliff face retreat exceeds cliff top retreat, the cliff becomes more unstable, and vice versa.

6. Summary

The three LiDAR-based estimates of cliff retreat, using observations of the cliff top, cliff face, and cliff base, are all limited by the accuracy and density of the observations. Cliff face change estimation is mostly automated, but requires manually deleting erroneous change caused by vegetation or other artifacts (if these areas cannot be removed through automated procedures). Manually digitizing the cliff top and base locations is labor intensive, with substantial errors when there is not a clear slope change between the beach and cliff face, and between the cliff face and cliff top. However, recent advances in automated extraction of cliff top and base positions (i.e. Liu et al., 2009) show promise, and may eliminate the labor intensive manual digitizing methods. Overall, cliff face change estimates were the most informative because all cliff changes, including changes at the cliff top and base, are captured. The cliff face method is also the most automated, and positive and negative changes are easily separated. The cliff top method captures real retreat, but provides only a limited view of cliff evolution. The cliff base method measures changes from basal erosion, but is complicated by a sensitivity to talus and sand levels at the cliff base.

Acknowledgments

LiDAR surveys were sponsored by the U.S. Army Corps of Engineers as part of the Southern California Beach Processes Study. APY received

Post-Doctoral Scholar support from the California Department of Boating and Waterways Oceanography Program.

References

- Aubrey, D.G., Inman, D.L., Winant, C.D., 1980. The statistical prediction of beach changes in southern California. *Journal of Geophysical Research* 85, 3264–3276.
- Benumof, B.T., Griggs, G.B., 1999. The dependence of seacliff erosion rates, cliff material properties, and physical processes: Sand Diego County, California. *Shore and Beach* 67 (4), 29–41.
- Budetta, P., Galiotta, G., Santo, A., 2000. A methodology for the study of the relationship between cliff erosion and the mechanical strength of soils and rock masses. *Engineering Geology* 56, 243–256.
- California Coastal Records Project, 2008. Copyright © Kenneth and Gabrielle Adelman. www.californiaacoastline.org.
- Dornbusch, U., Robinson, D.A., Moses, C.A., Williams, R.B.G., 2008. Temporal and spatial variations of chalk cliff retreat in East Sussex, 1873 to 2001. *Marine Geology* 249, 271–282.
- Federal Geographic Data Committee, 1998. Geospatial positioning accuracy standards, FGDC-STD-007. 3-1998, 28 pp.
- Greenwood, R.O., Orford, J.D., 2008. Temporal patterns and processes of retreat of drumlin coastal cliff – Strangford Lough, Northern Ireland. *Geomorphology* 94, 153–169.
- Hapke, C., Richmond, B., 2002. The impact of climatic and seismic events on the short-term evolution of seacliffs based on 3-D mapping, northern Monterey Bay, California. *Marine Geology* 187, 259–278.
- Hapke, C.J., Reid, D., 2007. National assessment of shoreline change, part 4: historical coastal cliff retreat along the California coast. U.S. Geological Survey Open-file Report 2007-1133. 51 pp.
- Jones, D.G., Williams, A.T., 1991. Statistical analysis of factors influencing coastal erosion along a section of the west Wales coast, UK. *Earth Surface Process and Landforms* 23, 1123–1134.
- Kennedy, M.P., 1975. Geology of the San Diego metropolitan area, western area. California Division of Mines and Geology Bulletin 200, 56 pp.
- Kuhn, G.G., Shepard, F.P., 1984. Sea Cliffs, Beaches, and Coastal Valleys of San Diego County: Some Amazing Histories and Some Horrifying Implications. University of California Press, Berkeley, California. 193 pp.
- Liu, J.K., Li, R., Deshpande, S., Niu, X., Shih, T.Y., 2009. Estimation of blufflines using topographic Lidar data and orthoimages. *Photogrammetric Engineering and Remote Sensing* 75, 69–79.
- Moore, L.J., Benumof, B.T., Griggs, G.B., 1999. Coastal erosion hazards in Santa Cruz and San Diego Counties, California. In: Crowell, M., Leatherman, S.P. (Eds.), *Coastal Erosion Mapping and Management: Journal of Coastal Research* 16, vol. 28, pp. 121–139.
- Pierre, G., Lahousse, P., 2006. The role of groundwater in cliff instability: an example at Cape Blanc-Nez (Pas-de-Calais, France). *Earth Surface Process and Landforms* 31, 31–45.
- Rosser, N.J., Petley, D.N., Lim, M., Dunning, S.A., Allison, R.J., 2005. Terrestrial laser scanning for monitoring the process of hard rock coastal cliff erosion. *Quarterly Journal of Engineering Geology and Hydrogeology* 38, 363–375.
- Wilcock, P.R., Miller, D.S., Shea, R.H., Kerkin, R.T., 1998. Frequency of effective wave activity and the recession of coastal bluffs: Calvert Cliff, Maryland. *Journal of Coastal Research* 14, 256–268.
- Young, A.P., 2006. Quantifying short-term seacliff morphology of a developed coast: San Diego County, California. Ph.D. Dissertation, Jacobs School of Engineering, University of California San Diego.
- Young, A.P., Ashford, S.A., 2006a. Application of airborne LIDAR for seacliff volumetric change and beach sediment contributions. *Journal of Coastal Research* 22, 307–318.
- Young, A.P., Ashford, S.A., 2006b. Performance evaluation of seacliff erosion control methods. *Shore and Beach* 74, 16–24.
- Young, A.P., Ashford, S.A., 2007. Quantifying sub-regional seacliff erosion using mobile terrestrial LIDAR. *Shore and Beach* 75, 38–43.
- Young, A.P., Olsen, M.J., Driscoll, N., Flick, R.E., Gutierrez, R., Guza, R.T., Johnstone, E., Kuester, F., in press. Comparison of airborne and terrestrial LIDAR estimates of seacliff erosion in southern California. *Photogrammetric Engineering and Remote Sensing*.